EC
Journals.ASM.org

Characterization of the Chloroquine Resistance Transporter Homologue in *Toxoplasma gondii*

Sally D. Warring,[a]* Zhicheng Dou,[c] Vern B. Carruthers,[c] Geoffrey I. McFadden,[a] Giel G. van Dooren[b]

Plant Cell Biology Research Centre, School of Botany, University of Melbourne, Parkville, Victoria, Australia[a]; Research School of Biology, Australian National University, Canberra, Australia[b]; Department of Microbiology and Immunology, University of Michigan Medical School, Ann Arbor, Michigan, USA[c]

Mutations in the *Plasmodium falciparum* chloroquine resistance transporter (*Pf*CRT) protein confer resistance to the antimalarial drug chloroquine. *Pf*CRT localizes to the parasite digestive vacuole, the site of chloroquine action, where it mediates resistance by transporting chloroquine out of the digestive vacuole. *Pf*CRT belongs to a family of transporter proteins called the chloroquine resistance transporter family. CRT family proteins are found throughout the Apicomplexa, in some protists, and in plants. Despite the importance of *Pf*CRT in drug resistance, little is known about the evolution or native function of CRT proteins. The apicomplexan parasite *Toxoplasma gondii* contains one CRT family protein. We demonstrate that *T. gondii* CRT (*Tg*CRT) colocalizes with markers for the vacuolar (VAC) compartment in these parasites. The *Tg*CRT-containing VAC is a highly dynamic organelle, changing its morphology and protein composition between intracellular and extracellular forms of the parasite. Regulated knockdown of *Tg*CRT expression resulted in modest reduction in parasite fitness and swelling of the VAC, indicating that *Tg*CRT contributes to parasite growth and VAC physiology. Together, our findings provide new information on the role of CRT family proteins in apicomplexan parasites.

In the intraerythrocytic life stage, *Plasmodium falciparum* parasites make a living by gaining energy from serum-derived glucose and consuming hemoglobin from the host erythrocyte as a source of amino acids (1). The hemoglobin is endocytosed and transported to the parasite's digestive vacuole (DV), a lysosome-like compartment containing peptidases that break down hemoglobin protein into its constituent amino acids (2). This digestion process releases toxic heme subunits from the hemoglobin protein into the DV. The parasite detoxifies these subunits by incorporating them into an inert crystalline substance called hemozoin (3). The antimalarial drug chloroquine accumulates in this digestive vacuole, where it acts by interfering with heme detoxification. Chloroquine inhibits the formation of hemozoin, causing toxic heme subunits to build up within the DV, eventually resulting in parasite death (4).

Resistance to chloroquine is widespread and is mediated by mutations in the so-called *P. falciparum* chloroquine resistance transporter (*Pf*CRT) (5, 6). *Pf*CRT is a multipass membrane transporter that localizes to the DV (5). Mutant *Pf*CRT proteins are able to transport chloroquine out of the DV, removing it from its site of action and thereby ablating its toxic effects on the parasite (7). *Pf*CRT belongs to a family of transporter proteins called the CRT family, which is part of the large drug/metabolite transporter superfamily (8, 9). Homologues of *Pf*CRT are found in all apicomplexan parasites, as well as in a range of other protists and plants. The plant *Arabidopsis thaliana* contains three *Pf*CRT homologues called chloroquinelike transporters (CLT) (10). These homologues localize to the *A. thaliana* plastid and regulate glutathione metabolism, likely by transporting glutathione and γ-glutamylcysteine between the cytoplasm and the plastid lumen (10).

The apicomplexan parasite *Toxoplasma gondii* contains one homolog of *Pf*CRT (*Tg*CRT). Like *A. thaliana*, both *P. falciparum* and *T. gondii* possess a plastid, termed the apicoplast. Unlike *P. falciparum*, *T. gondii* does not contain a large digestive vacuole, and the extent to which *T. gondii* uses endocytosis to sequester metabolites from its host cell in a manner akin to *Plasmodium* remains unclear.

In the work described in this paper, we investigated the localization and function(s) of *Tg*CRT to gain insights into the evolution and role of this family of transporters. We demonstrated that, in intracellular parasites, *Tg*CRT localized to highly dynamic vesicles that overlapped the markers for a lysosome-like vacuolar compartment called the VAC (11). In extracellular parasites, *Tg*CRT localized to one or a few larger, vacuole-like compartments that also overlapped the VAC markers. We generated a regulatable knockdown of *Tg*CRT expression and demonstrated that, while *Tg*CRT was not essential to the growth of *T. gondii in vitro*, the loss of *Tg*CRT resulted in a reduction in parasite fitness and dilation of the VAC compartment.

MATERIALS AND METHODS

Identification of *Tg*CRT. A BLASTP sequence similarity search using *Pf*CRT (accession number PF3D7_07090000, available at www.plasmodb.org) as a query sequence identified the *Tg*CRT genomic locus. This region partially corresponds to that encoded by the annotated gene TGME49_313930 (www.toxodb.org). Alignment of the predicted sequence to those of other CRT-like proteins suggested the gene model was incorrect. We therefore designed the primers 5′-ACTGCTCCACTGTTTTGCTTCG and 5′-GACATGGCTGTAAAGGTCTTCGC to amplify the entire open reading frame of *Tg*CRT by PCR, using cDNA from RHΔHXGPRT strain

Received 22 January 2014 Accepted 18 May 2014
Published ahead of print 23 May 2014
Address correspondence to Giel G. van Dooren, giel.vandooren@anu.edu.au.
* Present address: Sally D. Warring, Department of Biology, New York University, New York, New York, USA.
Supplemental material for this article may be found at http://dx.doi.org/10.1128/EC.00027-14.

doi:10.1128/EC.00027-14

T. gondii parasites as the template. We cloned and sequenced the resulting PCR product.

Alignment and phylogenetic analysis. CRT homologues from a range of organisms were identified by a BLASTP sequence similarity search with *Pf*CRT as the query sequence. We generated an initial alignment using ClustalX 2.0.12 (12), followed by manual adjustment in JALVIEW version 11.0 (13). The maximum likelihood tree was created using PhyML version 3.0 (14).

Plasmid construction and parasite transfections. Details on the construction of the various plasmids generated in this study, the selection procedures to generate the various parasite strains, and the Southern blotting approach are presented in the supplemental material.

Parasite culturing. Parasites were cultured in human foreskin fibroblast (HFF) cells grown in Dulbecco's modified Eagle's medium supplemented with 1% fetal calf serum and antibiotics. Where relevant, we added anhydrotetracycline (ATc) to a final concentration of 0.5 μg/ml.

SDS-PAGE and Western blotting. SDS-PAGE and Western blotting were performed as described previously (15). Membranes were probed with the following primary antibodies: rat antihemagglutinin (anti-HA) antibody (clone 3F10, 1:1,000 dilution; Roche Applied Science), mouse anti-green fluorescent protein (GFP) antibody (1:1,000; BD Biosciences), rabbit anti-*Tg*TOM40 antibody (1:1,000) (G.G.V.D., unpublished data), rabbit anti-*Tg*CPN60 antibody (1:5,000) (16), and mouse anti-*Tg*GRA8 antibody (1:100,000) (a kind gift from Gary Ward, University of Vermont) (17). We then probed with the following secondary antibodies: anti-rabbit horseradish peroxidase (HRP) antibody (1:10,000), anti-rat HRP antibody (1:1,000), and anti-mouse HRP antibody (1:200). Protein bands were visualized using the Amersham ECL plus Western blotting detection system (GE Healthcare). The mass of each band was calculated from an R_f plot.

To generate antibodies specific to *Tg*CRT, we PCR amplified a region encompassing the C-terminal 198 amino acids of the *Tg*CRT protein using the primers 5′-GGGTCCTGGTTCGATGATCATGAAACGGCG CGCC and 5′-CTTGTTCGTGCTGTTTATTATATACATCCGTTGTT CGC. We inserted the resultant fragment into the pAVA421 vector (18) by ligation-independent cloning and introduced the plasmid into *Escherichia coli* strain BL21. The recombinant protein was purified by affinity chromatography using a Ni-nitrilotriacetic acid (NTA) agarose resin (Qiagen). We generated polyclonal antiserum by inoculation into rabbits (Institute of Medical and Veterinary Science, Adelaide, South Australia). We used the antibody for Western blotting at a 1:200 dilution.

Sodium carbonate analysis. Intact membranes were isolated from clonal parasites expressing *Tg*CRT with a 3-HA epitope tag (*Tg*CRT-HA_3) by incubation in 100 mM Na_2CO_3 at pH 11.5 as described previously (15). Proteins extracted from both the membrane and soluble fraction were analyzed by SDS-PAGE and Western blotting as described previously (15).

Microscopy. Immunofluorescence assays were performed as described previously (15). The primary antibodies were rat anti-HA antibody (clone 3F10, 1:100 dilution; Roche Applied Science), mouse anti-*c*-myc antibody (clone 9E10, 1:200; Thermo Scientific), rabbit anti-*T. gondii* vacuolar pyrophosphatase-1 (*Tg*VP1) antibody (1:4,000; a kind gift from Silvia Moreno, University of Georgia), guinea pig anti-*T. gondii* Na^+/H^+ exchanger 3 (*Tg*NHE3) antibody (1:500; a kind gift from Gustavo Arrizabalaga, Indiana University), rabbit anti-*Tg*TOM40 antibody (1:2,000) (G.G.V.D., unpublished data), rabbit anti-*Tg*CPN60 antibody (1:1,000), mouse anti-*Tg*GRA8 antibody (1:100,000) (a kind gift from Gary Ward, University of Vermont) (17), mouse anti-*T. gondii* inner membrane complex (*Tg*IMC) antibody (monoclonal antibody 45.36, 1:1,000; a kind gift from Gary Ward, University of Vermont), rabbit anti-*Tg*MIC5 antibody (1:500) (19), and affinity-purified rabbit anti-*Tg*CPL antibody (1:100) (11). Secondary antibodies were anti-rat Alexa Fluor 488, anti-mouse Alexa Fluor 546, anti-guinea pig Alexa Fluor 594, anti-rabbit Alexa Fluor 546, and anti-rabbit Alexa Fluor 594 antibodies (1:200 to 1:500; Life Technologies). Images were acquired on a Leica TCS SP2 inverted laser-scanning confocal microscope or a Zeiss Axiovert Observer fluorescence microscope and linearly adjusted for contrast and brightness. For extracellular immunofluorescence assays, free parasites were fixed in 3% paraformaldehyde, affixed to coverslips using 0.1% polyethyleneimine, and then prepared as described above.

For live-cell imaging, freshly lysed *Tg*CRT-GFP-expressing parasites were allowed to invade human foreskin fibroblast cells grown to confluence on coverslips. The parasites were grown in standard growth medium overnight and then washed with growth medium to remove any remaining extracellular parasites. Images were taken on a Leica TCS SP2 inverted laser-scanning confocal microscope. For time-lapse imaging, parasites were allowed to invade a host cell monolayer grown in glass bottom dishes (MatTek) for 1 h. The sample was washed three times and replaced with Evrogen antibleaching live-cell visualization medium (20). Images were taken at 15-min intervals using a Zeiss Axiovert Observer inverted fluorescence microscope. Cultures were maintained in a humidified environment at 37°C with 5 to 10% CO_2 in air for the duration of imaging.

Parasite growth and competition assays. To measure parasite growth, we performed plaque assays by adding 200 parasites to a 25-cm^2 tissue culture flask containing a confluent monolayer of human foreskin fibroblasts in the absence or presence of ATc. We grew parasites undisturbed for 9 days and performed plaque assays as described previously (15). The plaque areas were determined for approximately 50 plaques from each flask, and *P* values were calculated using a 2-tailed unpaired Student's *t* test. As a more quantitative measure of parasite growth, we introduced a tandem-dimeric Tomato (tdTomato) red fluorescent protein into i*Tg*CRT/Δ*Tg*CRT parasites (described below) by electroporation and selected for parasites expressing the tdTomato RFP transgene by flow cytometry (15). Flow cytometry was performed at the John Curtin School of Medical Research (Australian National University). We measured parasite growth in the absence or presence of ATc using a Fluostar Optima fluorescence plate reader as described previously (15, 21).

Competition assays were performed in triplicate by mixing mutant i*Tg*CRT/Δ*Tg*CRT parasites with parental i*Tg*CRT/e*Tg*CRT parasites (described below) at a 1:1 ratio. The mixed culture was added to 25-cm^2 tissue culture flasks containing confluent human foreskin fibroblasts in the presence or absence of ATc. Cultures were passed every 4 days, and immunofluorescence assays were performed every second pass. One hundred vacuoles were counted from each culture, and the experiment was performed in triplicate. Mutant parasites were distinguished from parental parasites by labeling with mouse anti-chloramphenicol acetyltransferase (CAT) antibodies (Abcam), with the CAT protein only present in *iTg*CRT/Δ*Tg*CRT strain parasites.

Quantification of VAC size. Wild-type (RH) and i*Tg*CRT/Δ*Tg*CRT parasites were treated with 0.5 μg/ml ATc for 2 days. Freshly lysed parasites were added to HFF cells, allowed to settle for 15 min at room temperature, and then incubated at 37°C for 30 min for invasion. Noninvaded parasites were washed away with phosphate-buffered saline. Infected HFF cells were fixed with 4% paraformaldehyde and stained with affinity-purified rabbit anti-*Tg*CPL antibodies (11) at a 1:100 dilution. Images were captured with a Zeiss Axiovert Observer Z1 inverted fluorescence microscope equipped with a 100×, 1.3-numerical-aperture objective lens and an AxioCAM MRm camera. The diameters of VAC compartments were quantified using Zeiss Axiovision 4.3 software. For nonspherical VACs, we measured the widest diameter. *P* values were calculated using an unpaired Student's *t* test.

GenBank nucleotide sequence accession number. The corrected *Tg*CRT cDNA sequence has been deposited in GenBank under accession number KJ130040.

RESULTS

***T. gondii* contains one CRT family protein.** To identify possible homologues of *Pf*CRT in *Toxoplasma gondii*, we performed BLAST searches of the *T. gondii* genome (www.toxodb.org) using *Pf*CRT as a query sequence. We identified a single putative CRT homologue encoded on chromosome XI and called this *Tg*CRT. This

corresponded to a gene previously included in an alignment of CRTs from a range of organisms (22). To determine the correct coding sequence of *Tg*CRT, we amplified the entire open reading frame, using cDNA as a template. This revealed that the *Tg*CRT model presented in toxoDB is incorrect. The correct sequence encodes a protein of 890 amino acids, with a predicted mass of 92 kDa.

To elucidate the evolutionary relationships between CRT family proteins, we performed a phylogenetic analysis on CRT family proteins from apicomplexans, oomycetes, plants, red algae, and amoebae. This revealed that *Tg*CRT branches with CRT homologues from related coccidian parasites, such as *Eimeria tenella* and *Neospora caninum* (see Fig. S1A in the supplemental material). We identified single CRT family proteins from each apicomplexan parasite that we examined, but the phylogenetic tree was not sufficiently resolved to determine whether these represent a monophyletic group. A multiple sequence alignment (see Fig. S1B) reveals that the similarity of *Tg*CRT to other CRT family proteins resides in the central region of the protein, which spans the 10 predicted transmembrane helices. Compared to CRT family proteins from other organisms, coccidian CRT proteins harbor extended N and C termini (see Fig. S1C). A key mutation that confers chloroquine resistance in *Pf*CRT is the conversion of lysine 76 to a threonine (K76T) (5, 23). Intriguingly, *Tg*CRT and other coccidian CRTs harbor a threonine in this position (see Fig. S1B). *Tg*CRT, however, resembles wild-type *Pf*CRT at several other positions with a known role in conferring chloroquine transport activity, such as N76 and N326 (see Fig. S1B) (23). *Tg*CRT contains numerous other regions that are conserved in CRT homologues from other organisms, including a cysteine-rich motif in the loop between transmembrane domains 7 and 8 (see Fig. S1D).

***Tg*CRT localizes to a population of dynamic vesicles.** To examine the localization of *Tg*CRT, we inserted an HA_3 epitope tag at the 3′ end of the native *Tg*CRT open reading frame in Δ*ku80 T. gondii* parasites (24, 25). We observed *Tg*CRT-HA_3 localizing to multiple small puncta in intracellular parasites (Fig. 1A). Western blot analysis of the resulting cell line revealed a protein with an observed mass of 87 kDa (Fig. 1B), congruent with the predicted mass of 92 kDa. Like other CRT family proteins, *Tg*CRT contains multiple predicted transmembrane domains (see Fig. S1B and C in the supplemental material). To establish whether *Tg*CRT is a membrane-bound protein, we carried out a Na_2CO_3 partitioning assay on the parasite line expressing *Tg*CRT-HA_3 (26). This assay segregates integral membrane proteins from soluble and peripheral membrane proteins. *Tg*CRT-HA_3 partitioned into the integral membrane fraction (Fig. 1C), consistent with *Tg*CRT being a transmembrane protein. We conclude that *Tg*CRT is an integral membrane protein that resides in small, membrane-bound vesicles in intracellular parasites.

To investigate the identity of the putative *Tg*CRT-containing vesicles, we colabeled *Tg*CRT-HA_3 with markers for several well-described organelles in *T. gondii* tachyzoites, including the apicoplast, mitochondrion, dense granules, and micronemes (Fig. 2A to D). *Tg*CRT-HA_3 did not colocalize with any of these markers.

Earlier studies revealed that the proton-pumping vacuolar ATPase of *T. gondii* (*Tg*V-ATP) localizes to small vesicles that were described as acidocalcisomes (27). To determine whether *Tg*CRT colocalizes with *Tg*V-ATP, we inserted a *c*-myc epitope tag into the 3′ end of the open reading frame of subunit B of the V-ATP (*Tg*V-ATP-cmyc). We transfected this construct into the parasite line already expressing *Tg*CRT-HA_3. Immunofluorescence assays carried out on the resulting parasite line showed that *Tg*CRT-HA_3 and *Tg*V-ATP-cmyc partially overlap in intracellular tachyzoites (Fig. 2E, arrowheads). We next colabeled *Tg*CRT-HA_3 with antibodies against vacuolar pyrophosphatase-1 (*Tg*VP1), a marker for the late endosomes in intracellular parasites (11, 28). We observed essentially no overlap between these structures (Fig. 2F). As a second marker for late endosomes, we colabeled *Tg*CRT-HA_3 parasites with antibodies against *Tg*NHE3, a Na^+/H^+ exchanger (29). Again, we observed no overlap between these organelles (Fig. 2G).

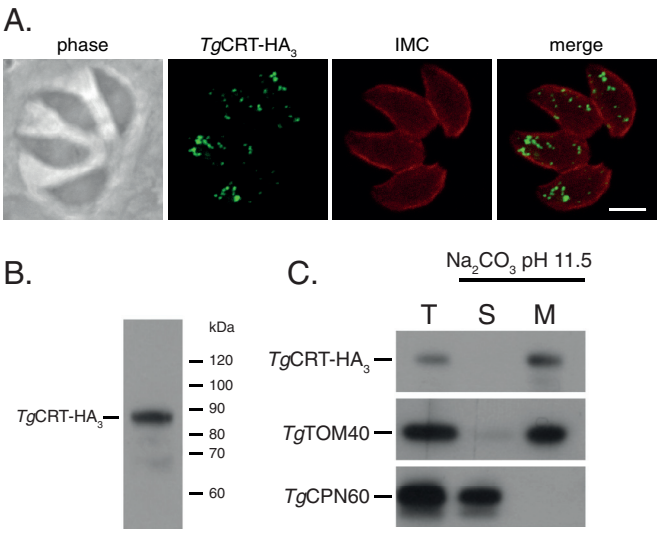

FIG 1 *Tg*CRT is an integral membrane protein that localizes to multiple vesicles in intracellular parasites. (A) Immunofluorescence assay of cells expressing C-terminally tagged native *Tg*CRT (*Tg*CRT-HA_3) labeled with antibodies against the HA epitope (green) and the inner membrane complex (IMC; red). Scale bar, 3 μm. (B) Anti-HA Western blot of cell line expressing *Tg*CRT-HA_3, revealing a single protein band of an estimated 87 kDa. (C) Western blot of a sodium carbonate extraction of *Tg*CRT-HA_3-expressing parasites showing total (T), soluble (S), and membrane (M) proteins. *Tg*CRT partitions into the membrane fraction. *Tg*TOM40 and *Tg*CPN60 are used as controls for membrane and soluble proteins, respectively.

The vesicular pattern of *Tg*CRT labeling resembled that of the fragmented VAC compartment described in intracellular parasites (11). We therefore colabeled *Tg*CRT-HA_3-expressing parasites with antibodies against *Tg*CPL, a marker for the VAC. This revealed considerable overlap between the two compartments (Fig. 2H), suggesting that *Tg*CRT is associated with the VAC.

***Tg*CRT-containing organelles change morphology in extracellular parasites.** The lytic cycle of *T. gondii* alternates between intracellular dividing cells and motile extracellular stages. The VAC is highly dynamic in intracellular tachyzoites (11). During most stages of the parasite lytic cycle, the VAC is fragmented into multiple smaller vesicular structures, but it is seen as one or more larger vacuolar structures in extracellular parasites. To observe *Tg*CRT localization in extracellular parasites, we performed immunofluorescence assays on parasites expressing *Tg*CRT-HA_3 and *Tg*V-ATP-cmyc (Fig. 3A) or on *Tg*CRT-HA_3-expressing parasites colabeled with antibodies against *Tg*VP1 (Fig. 3B), *Tg*NHE3 (Fig. 3C), or *Tg*CPL (Fig. 3D). Interestingly, the morphology of the *Tg*CRT-containing compartment is markedly different in extracellular tachyzoites. Consistent with previous observations of the VAC (11), *Tg*CRT-HA_3 localization appears as one or a few

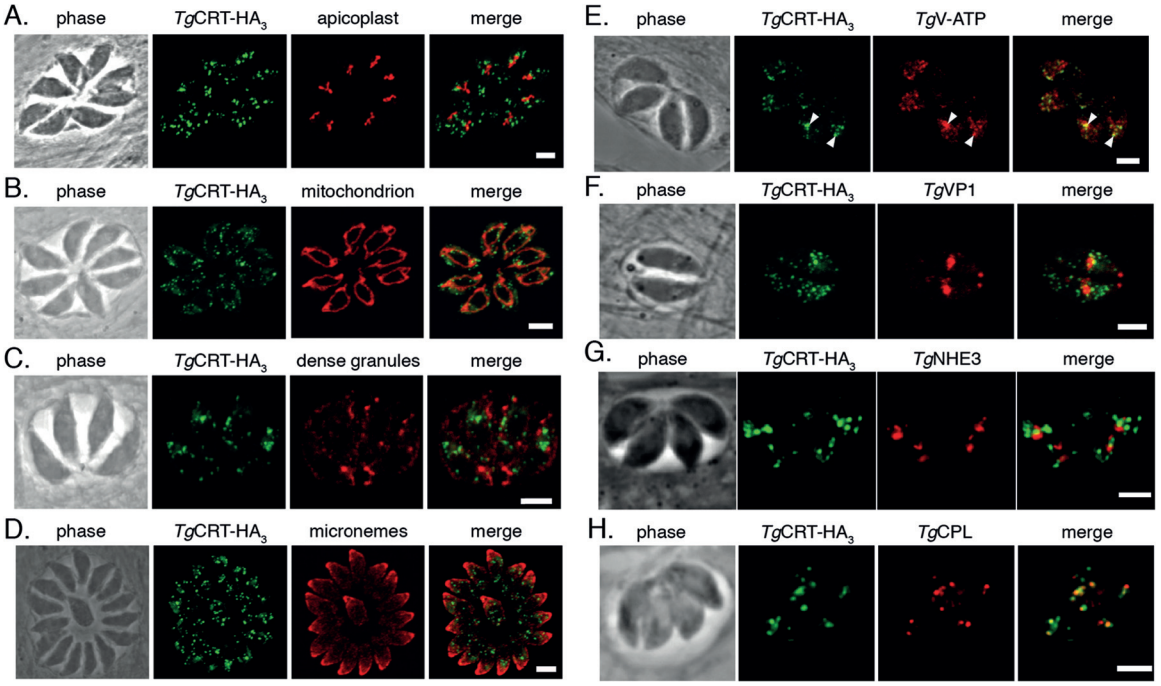

FIG 2 *Tg*CRT colocalizes with the *T. gondii* vacuole (VAC) compartment. Immunofluorescence assays of cell lines expressing *Tg*CRT-HA$_3$, labeled with anti-HA antibody (green) and colabeled with anti-*Tg*CPN60 antibody (red) to identify the apicoplast (A), anti-*Tg*TOM40 antibody to identify the mitochondrion (B), anti-*Tg*GRA8 antibody to identify the dense granules (C), anti-*Tg*MIC5 antibody to identify the micronemes (D), anti-*c*-myc antibody to identify C-terminally *c*-myc-tagged subunit B of *Tg*V-ATP (arrowheads indicate points of colocalization with *Tg*CRT-HA$_3$) (E), anti-*Tg*VP1 antibody to identify the PLV/late endosomes (F), anti-*Tg*NHE3 antibody as a further marker for the PLV (G), and anti-*Tg*CPL antibody to identify the VAC (H). Scale bars, 3 μm.

larger vacuolar organelles in extracellular parasites (Fig. 3). Conversely, *Tg*V-ATP-cmyc appears to localize to the plasma membrane and cytoplasm rather than to any defined vesicular structures (Fig. 3A).

Previous studies have defined *Tg*VP1 and *Tg*NHE3 as markers for the plant-like vacuole (PLV) (28, 29) in extracellular parasites. We find that *Tg*VP1 and *Tg*NHE3 localize to a large vacuolar structure in extracellular parasites that shows a close spatial association with the *Tg*CRT-HA$_3$ localization (Fig. 3B and C), although in our hands, these structures are not overlapping. *Tg*CRT and *Tg*CPL retain their colocalization in extracellular parasites (Fig. 3D), consistent with *Tg*CRT localization to the VAC.

To further explore the change in morphology between extracellular and intracellular tachyzoites, we generated a parasite line where *Tg*CRT was fused to green fluorescent protein (GFP). This allowed us to visualize the VAC in live parasites. Live-cell fluorescence images of intracellular *T. gondii* expressing *Tg*CRT-GFP reveal the presence of multiple small vesicles in intracellular parasites (Fig. 4A), mirroring what we observed in epitope-tagged parasites. In extracellular parasites, *Tg*CRT-GFP localizes to a larger vesicle and, occasionally, some smaller vesicles (Fig. 4B). Western blotting reveals that *Tg*CRT-GFP exists as a single protein of 120 kDa, similar to the predicted mass of 124 kDa (Fig. 4C).

Having established *Tg*CRT-GFP as a robust marker for the VAC compartment in live parasites, we next set out to characterize the dynamics of the changes that occur in this compartment between extra- and intracellular stages by performing time-lapse imaging of *Tg*CRT-GFP parasites. We allowed parasites to invade host cells and then imaged single-cell vacuoles every 15 min for 7 h (Fig. 4D; see also Movie S1 in the supplemental material). During this time frame of intracellular growth, the large VAC compartment observed in extracellular parasites fragments substantially. Notably, the VAC is fragmented before the parasite undergoes its first round of cell division (Fig. 4D). To quantify fragmentation of the VAC, we counted *Tg*CRT-GFP-containing vesicles in parasites at regular time intervals postinvasion (Fig. 4E). In extracellular parasites (time zero), *Tg*CRT-GFP exists in an average of approximately three separate compartments, typically one larger compartment and some smaller ones. Eight hours postinvasion, parasites typically have over a dozen smaller *Tg*CRT-GFP-containing vesicles. The relationship between vesicle number and time postinvasion has a statistically significant Spearman's rank correlation coefficient of 0.752 ($P < 0.0001$), suggesting a strong correlation between time after invasion and vesicle number.

The role of *Tg*CRT in parasite fitness and VAC morphology. *Pf*CRT has proven recalcitrant to genetic ablation, suggesting that it may be essential to parasite survival (30). To determine whether *Tg*CRT is important for growth in *T. gondii*, we first generated a parasite strain expressing an anhydrotetracycline (ATc)-regulated *Tg*CRT gene in TATi strain *T. gondii* parasites (31). This parental cell line, termed i*Tg*CRT/e*Tg*CRT, expresses both native and ATc-regulatable copies of *Tg*CRT. We then deleted the 5′ region of the native *Tg*CRT locus by double homologous recombination, using a previously described cosmid recombineering system (32) to generate a parasite line, termed i*Tg*CRT/Δ*Tg*CRT, that expresses only the ATc-regulatable copy of *Tg*CRT. Southern blot analysis of the resulting cell line demonstrated successful disruption of the native *Tg*CRT locus (see Fig. S2 in the supplemental material).

To measure the regulation of *Tg*CRT in the i*Tg*CRT/Δ*Tg*CRT

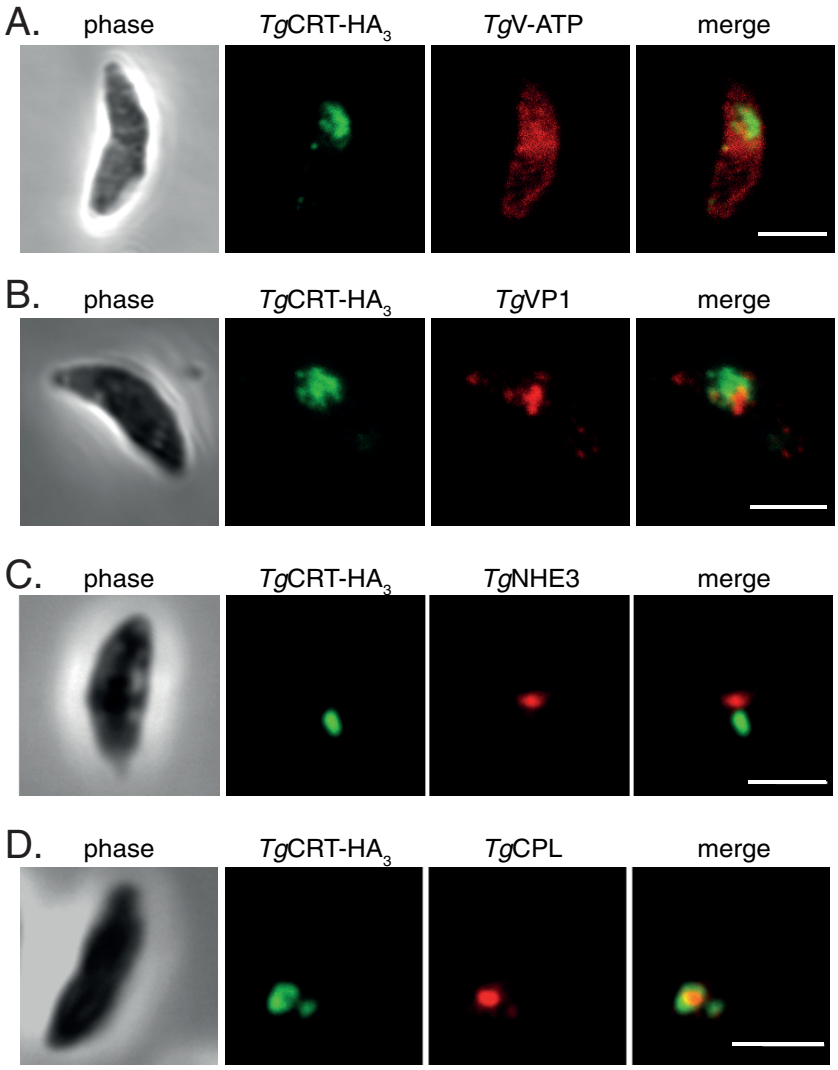

FIG 3 *Tg*CRT-containing vesicles change their morphology in extracellular parasites. Immunofluorescence assays of extracellular parasites expressing *Tg*CRT-HA_3, colabeled with antibodies against *Tg*V-ATP (A), *Tg*VP1, a marker for the PLV (B), *Tg*NHE3, a second marker for the PLV (C), and *Tg*CPL, a marker for the VAC (D). Scale bars, 3 μm.

cell line, we incubated parasites in the absence of ATc (day 0) or the presence of ATc for 1, 2, and 3 days and then performed Western blotting to detect the HA-tagged *Tg*CRT protein. After 1 day on ATc, *Tg*CRT levels are greatly reduced, and after 2 days, the protein is undetectable (Fig. 5A), demonstrating robust downregulation of the protein in the i*Tg*CRT/Δ*Tg*CRT cell line. To compare the levels of ATc-regulated *Tg*CRT expression to the wild-type *Tg*CRT level, we generated polyclonal antibodies against *Tg*CRT and probed proteins extracted from i*Tg*CRT/e*Tg*CRT and i*Tg*CRT/Δ*Tg*CRT cell lines grown with and without ATc. In the absence of ATc in both cell lines, we observed bands of the expected mass for *Tg*CRT (Fig. 5B). When we knocked down i*Tg*CRT expression through the addition of ATc in the i*Tg*CRT/e*Tg*CRT cell line, we observed a band corresponding to the expected mass for native *Tg*CRT but at a reduced intensity compared to that obtained when the ATc-regulatable copy of *Tg*CRT is expressed (Fig. 5B). This suggests that there is overexpression of *Tg*CRT from the ATc-regulated promoter. Nevertheless, when we cultured i*Tg*CRT/Δ*Tg*CRT in the presence of ATc, *Tg*CRT protein was undetectable (Fig. 5B), indicating that the i*Tg*CRT/Δ*Tg*CRT strain allows strong depletion of *Tg*CRT protein upon the addition of ATc.

To elucidate the importance of *Tg*CRT for parasite growth and viability, we performed plaque assays on the i*Tg*CRT/Δ*Tg*CRT and i*Tg*CRT/e*Tg*CRT parasite lines. Parasites were added to a monolayer of human foreskin fibroblast cells and grown for 9 days in the presence or absence of ATc. Over this time, parasites will form zones of clearance in the host cell monolayer, which become apparent upon staining with crystal violet dye. The sizes of the plaques indicate how well the parasites have grown during this time. We found that i*Tg*CRT/Δ*Tg*CRT grew in both the absence and presence of ATc, suggesting that *Tg*CRT is not essential for parasite growth (Fig. 6A). Quantification of plaque size revealed that plaques of the i*Tg*CRT/Δ*Tg*CRT parasite line grown in the presence of ATc were on average smaller than those of i*Tg*CRT/Δ*Tg*CRT parasites grown in the absence of ATc ($P < 0.0001$)

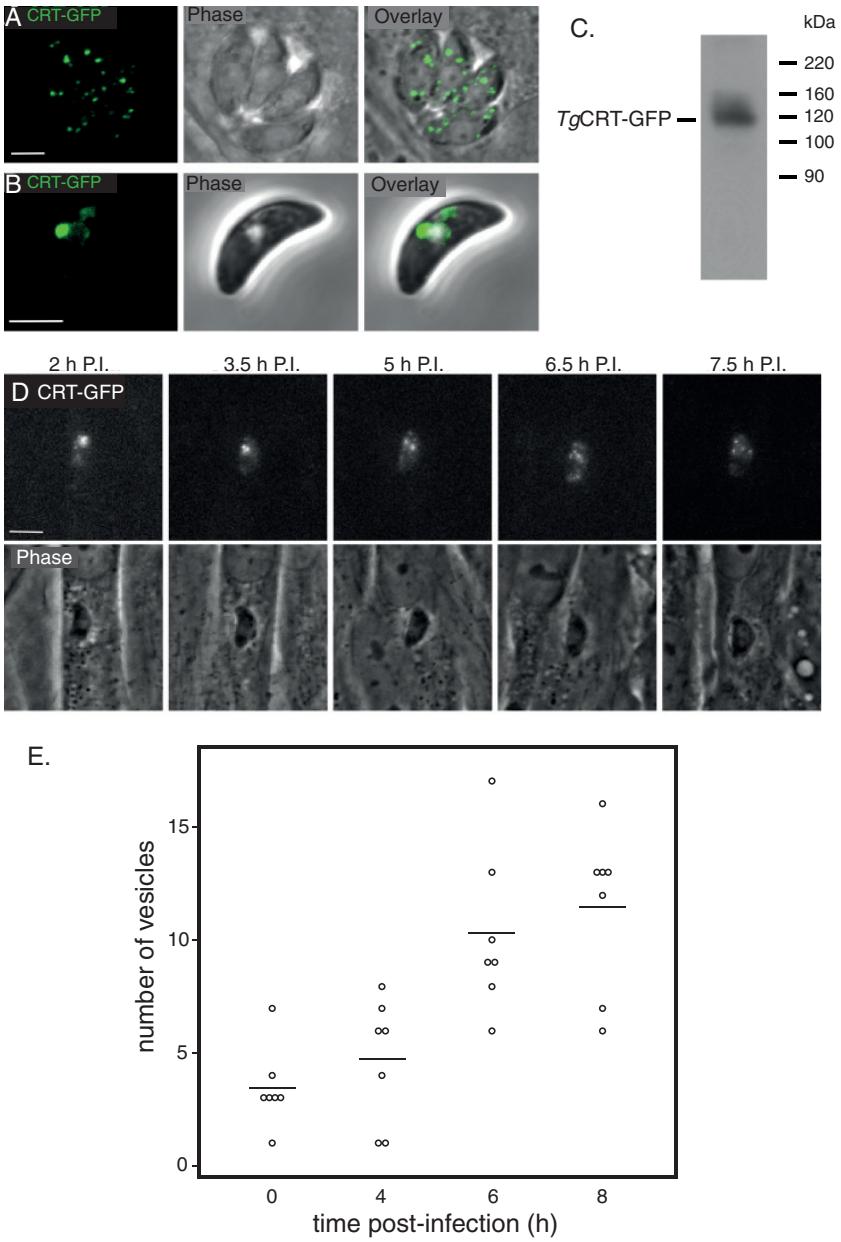

FIG 4 The large vacuole in extracellular parasites breaks down after host cell invasion. Live confocal images of intracellular (A) and extracellular (B) parasites expressing *Tg*CRT-GFP. (C) Anti-GFP Western blot of cell line expressing *Tg*CRT-GFP. *Tg*CRT-GFP appears as a band of approximately 120 kDa. (D) Individual frames from time-lapse imaging of a single live cell using fluorescence microscopy. Parasites expressing *Tg*CRT-GFP were allowed to invade host cells for 1 h and then imaged every 15 min postinvasion (P.I.). Scale bar, 3 μm. (E) Quantification of the numbers of CRT-containing vesicles in parasites at regular intervals postinvasion, represented as a dot plot.

(Fig. 6B). This effect is likely specifically due to the depletion of *Tg*CRT from this cell line, since we observed little difference in plaque size upon the addition of ATc to the parental i*Tg*CRT/e*Tg*CRT cell line ($P > 0.05$) (Fig. 6B).

As a more quantitative measure of parasite growth, we introduced a superbright tdTomato fluorescent protein into the i*Tg*CRT/Δ*Tg*CRT cell line. We added parasites to wells of a 96-well plate and measured the fluorescence intensity of each well on a daily basis, with the fluorescence in each well correlating directly to parasite growth (15, 21). The i*Tg*CRT/Δ*Tg*CRT parasites grew ~30% more slowly in the presence of ATc (Fig. 6C), again supporting a minor role for *Tg*CRT in parasite growth.

These data suggested a fitness cost associated with the loss of *Tg*CRT in *T. gondii* parasites. To test this, we performed a competition assay where parental i*Tg*CRT/e*Tg*CRT and i*Tg*CRT/Δ*Tg*CRT mutant parasites were mixed in a 1:1 ratio and then grown in the presence or absence of ATc. We could distinguish mutant from parental parasites by performing immunofluorescence assays to detect the presence of chloramphenicol acetyltransferase, which is only present in the mutant. We monitored the parasites over 24 days. During this time, the ratio of the two

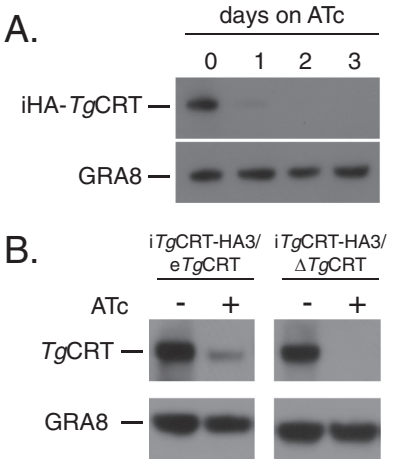

FIG 5 Regulatable knockdown of *Tg*CRT. (A) Western blot analysis of the i*Tg*CRT/Δ*Tg*CRT mutant cell line to determine the extent of i*Tg*CRT downregulation upon the addition of ATc. Parasites were grown from 0 to 3 days on ATc and probed with antibodies against iHA-*Tg*CRT, as well as antibodies against GRA8 as a loading control. (B) Western blot analysis of i*Tg*CRT/e*Tg*CRT and i*Tg*CRT/Δ*Tg*CRT cell lines grown in the absence and presence of ATc. Parasites were probed with anti-CRT antibodies, as well as anti-GRA8 antibodies as a loading control.

parasite strains grown in the absence of ATc remained approximately 1:1 (Fig. 6D). In contrast, i*Tg*CRT/Δ*Tg*CRT parasites were rapidly outcompeted in the presence of ATc, with less than 5% remaining after 24 days (Fig. 6D).

Our data indicate that *Tg*CRT is not essential for parasite growth but that loss of *Tg*CRT does incur a fitness cost on the parasite. We also demonstrate that *Tg*CRT localizes to the VAC compartment. We wondered whether loss of *Tg*CRT would result in morphological changes to the VAC. To test this, we performed immunofluorescence assays to label the VAC in wild-type (RH) and i*Tg*CRT/Δ*Tg*CRT parasites grown in the absence and presence of ATc. We focused on recently invaded parasites in which the VAC was still in its larger, extracellularlike form. We noted that the VAC appeared larger in parasites lacking *Tg*CRT (Fig. 7A). To quantify this, we measured the diameter of the VAC and found that the VAC of i*Tg*CRT/Δ*Tg*CRT parasites grown in the presence of ATc was on average 1.3 μm in diameter, significantly larger than the average 0.73-μm diameter found in parasites grown without ATc (Fig. 7B) ($P < 0.0001$). We observed no such difference in wild-type parasites. Together, these results suggest that the loss of *Tg*CRT leads to an enlargement of the VAC compartment, suggesting an effect on the physiology of this organelle.

DISCUSSION

The CRT protein family is found in a diverse array of eukaryotes. In plants, chloroquine-like transporters localize to the plastid, where they appear to play a role in glutathione homeostasis and metabolism, possibly by mediating glutathione export from the organelle (10). In erythrocytic stages of *Plasmodium*, CRT proteins localize to the digestive vacuole (DV) (5), a lysosome-like organelle that functions primarily in the digestion of hemoglobin (33, 34). The DV houses a suite of proteases that digest hemoglobin into its constituent amino acids, which are then utilized for parasite growth (1, 33). In *Plasmodium*, chloroquine accumulates in the DV and interferes with the polymerization of heme released from hemoglobin (4, 35). Heme in its free state is highly toxic to the parasite (36). Failure to polymerize heme results in swelling of the DV and rapid parasite death (37, 38). Mutant CRT alleles in *P. falciparum* confer resistance to the major antimalarial drug chloroquine by transporting chloroquine from the DV (5, 7).

In this study, we characterized the CRT homologue from the model apicomplexan *T. gondii*, revealing that *Tg*CRT localizes to the recently described VAC compartment (11). The VAC is a proteolytic compartment that houses cathepsin-like cysteine proteases, such as *Tg*CPL and *Tg*CPB (11, 39). Using a live-cell-imaging approach, we demonstrated that the VAC is a highly dynamic compartment. In extracellular and recently invaded parasites, it typically exists as a single large compartment, which then apparently fragments into a dozen or more smaller *Tg*CRT-containing vesicles during parasite replication.

We demonstrate here that the *Tg*CRT-labeled VAC is distinct from the plant-like vacuole (PLV) in intra- and extracellular parasites. *Tg*VP1 was described as the seminal marker of the PLV in *T. gondii* (28). In a parallel study, *Tg*CPL was reported to be a marker of the VAC (11). Both studies reported that intracellular replicating parasites show *Tg*VP1 associated with markers of late endosomes, whereas *Tg*CPL was seen in multiple vesicular structures attributed to fragmentation of the resident organelle (11, 28). However, in extracellular parasites, these markers were reported to colocalize in the PLV in one study (28) but were observed separately in the VAC (*Tg*CPL) and late endosome (*Tg*VP1) in the parallel study (11). The discrepant findings were attributed to the dynamic nature of these endolysosomal organelles and possible fusion of the VAC with late endosomes to form the PLV. Regardless, these studies provided evidence for multiple functions of the PLV and VAC organelles, including roles in regulating ion balance in response to changes in the extracellular environment and proteolytic processing or digestion of proteins. In this study, we have used the term VAC when referring to a compartment(s) associated with *Tg*CPL, while PLV has been used to indicate structures associated with *Tg*VP1.

The proteomic makeup of the VAC appears quite dynamic. The vacuolar H^+-pumping ATPase associates with some *Tg*CRT-containing vesicles in intracellular parasites, suggesting that these are acidic compartments. In extracellular parasites, however, the association between the VAC and the vacuolar H^+-pumping ATPase is not apparent. In a similar vein, a previous study demonstrated that *Tg*CPL and *Tg*CPB do not always colocalize to the same intracellular vesicles (39), and we find that the same is true of *Tg*CPL and *Tg*CRT (Fig. 2H). Notably, we find that *Tg*CRT does not overlap with *Tg*VP1 and *Tg*NHE3, markers for the PLV (28, 29). This is perhaps surprising, given that the PLV exists as a large vacuole in extracellular parasites that morphologically resembles the extracellular *Tg*CRT-containing vacuole (28). Clearly, more work is required to better define the protein composition and functions of both the *Tg*CRT-containing VAC compartment and the PLV.

The intracellular *Tg*CRT-associated VAC compartments exhibit numerous intriguing similarities to the DV of *Plasmodium* (Fig. 8). In addition to the presence of CRT homologues in both the VAC and DV, both compartments house cathepsin proteases, *Tg*CPL and *Tg*CPB in the case of the VAC and falcipains 2a, 2b, and 3 in the case of the DV (40). During intracellular replication, both compartments also harbor a V-type H^+-pumping ATPase that likely functions in maintaining the acidity of the organelle

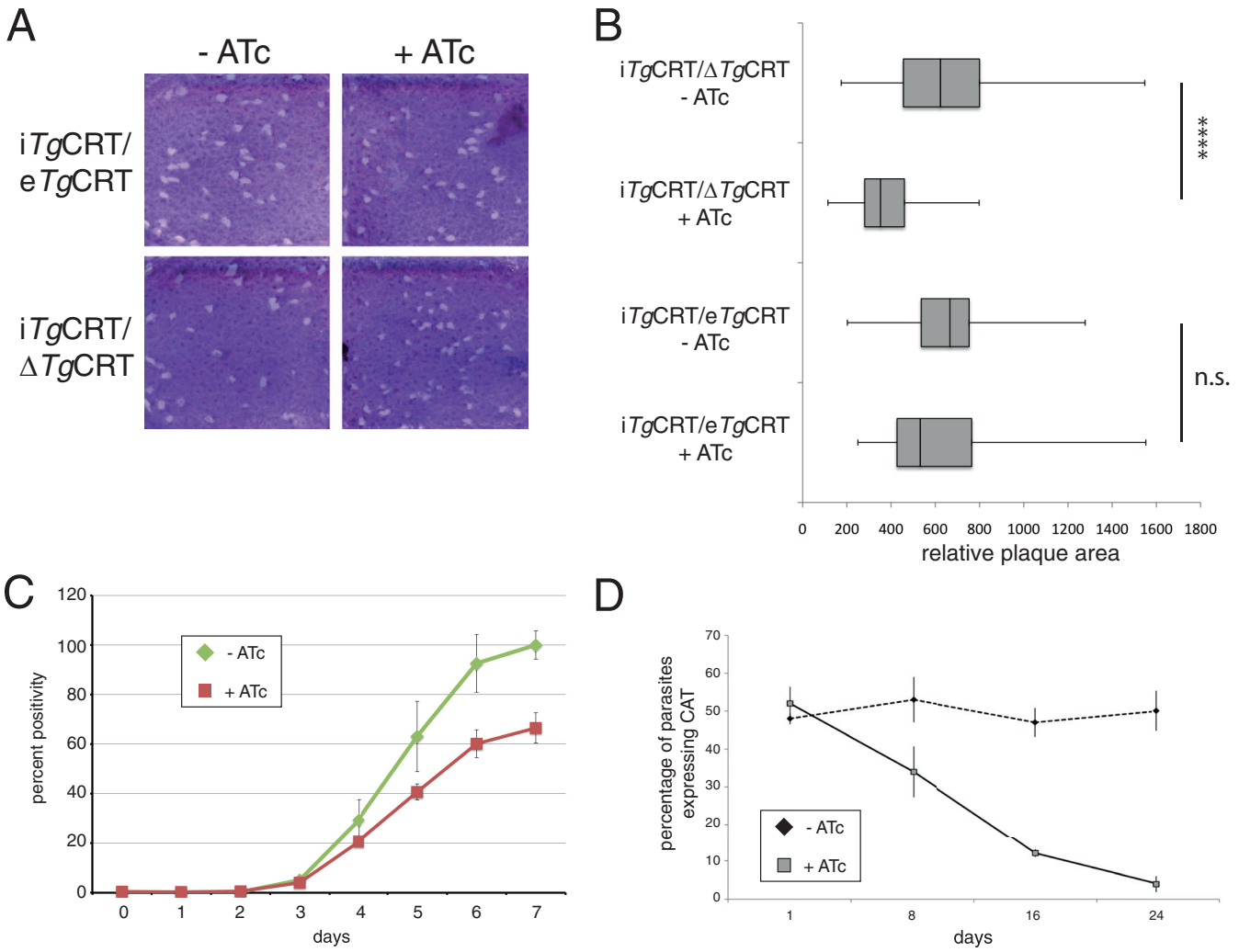

FIG 6 *Tg*CRT is not essential for *T. gondii* growth, but depletion of *Tg*CRT imparts a fitness cost on parasites. (A) Plaque assays of i*Tg*CRT/e*Tg*CRT and i*Tg*CRT/Δ*Tg*CRT cell lines grown in the absence and presence of ATc. (B) Quantification of the relative areas of plaques in the parental and mutant cell lines grown in the absence and presence of ATc. These are represented as box and whisker plots, with the medians indicated by vertical bars, the 1st and 3rd quartiles forming the box, and whiskers indicating the minimum and maximum values. ****, $P < 0.0001$; n.s., not significant. (C) Fluorescence growth assay of i*Tg*CRT/Δ*Tg*CRT parasites grown in the absence and presence of ATc over 7 days. Error bars each represent one standard deviation from the mean of three technical replicates. (D) Competition assay of i*Tg*CRT/e*Tg*CRT and i*Tg*CRT/Δ*Tg*CRT parasites grown in the absence and presence of ATc. Parasites were mixed in a 1:1 ratio at the start of the experiment, and the percentages of i*Tg*CRT/Δ*Tg*CRT parasites in the population were monitored over 24 days, as a percentage of parasites expressing the CAT protein. Error bars each indicate one standard deviation from the mean.

(41). Given these similarities, we hypothesize that the common ancestor of *Plasmodium* and *Toxoplasma* may have harbored an acidic lysosome-like vacuole that gave rise to the VAC in *T. gondii* and the DV in *Plasmodium* (Fig. 8).

Despite this possible shared ancestry, some of the functions of the DV and VAC differ in their respective parasites. The DV of *Plasmodium* functions primarily in the proteolytic digestion of hemoglobin. Endocytic vesicles carrying hemoglobin from the erythrocyte form at a cytosome and are internalized into the parasite (42). These endocytic vesicles are acidified and contain proteases that can digest hemoglobin. Ultimately, the endocytic vesicles fuse to form the larger DV, where the bulk of hemoglobin digestion in the parasite takes place (42). There is currently limited evidence that tachyzoites of *T. gondii* perform endocytosis. The function of proteases, such as *Tg*CPL and *Tg*CPB, and the functions of the VAC more generally remain poorly defined. Knockout of *Tg*CPL partially impairs the proteolytic maturation of *Tg*CPB and certain microneme proteins, suggesting a role in protein activation (11, 39). While falcipains are maturases for plasmepsin aspartyl proteases in the DV (43), they have not been linked to the maturation of microneme proteins. Our hypothesis that the *T. gondii* VAC and the *Plasmodium* DV are homologous organelles may provide a framework for understanding possible functions of the VAC, although much research remains to confirm the evolutionary link between these organelles.

Although the role of mutant *Pf*CRT alleles in chloroquine transport is clear (7), the native function of CRT homologues in apicomplexans remains to be elucidated. Unpublished attempts to knock out *Pf*CRT were unsuccessful (30), suggesting that *Pf*CRT may be essential for *P. falciparum* survival in erythrocytic stages. Knockdown of chloroquine-resistant *Pf*CRT protein levels to approximately 65% of the wild-type levels lessened parasite

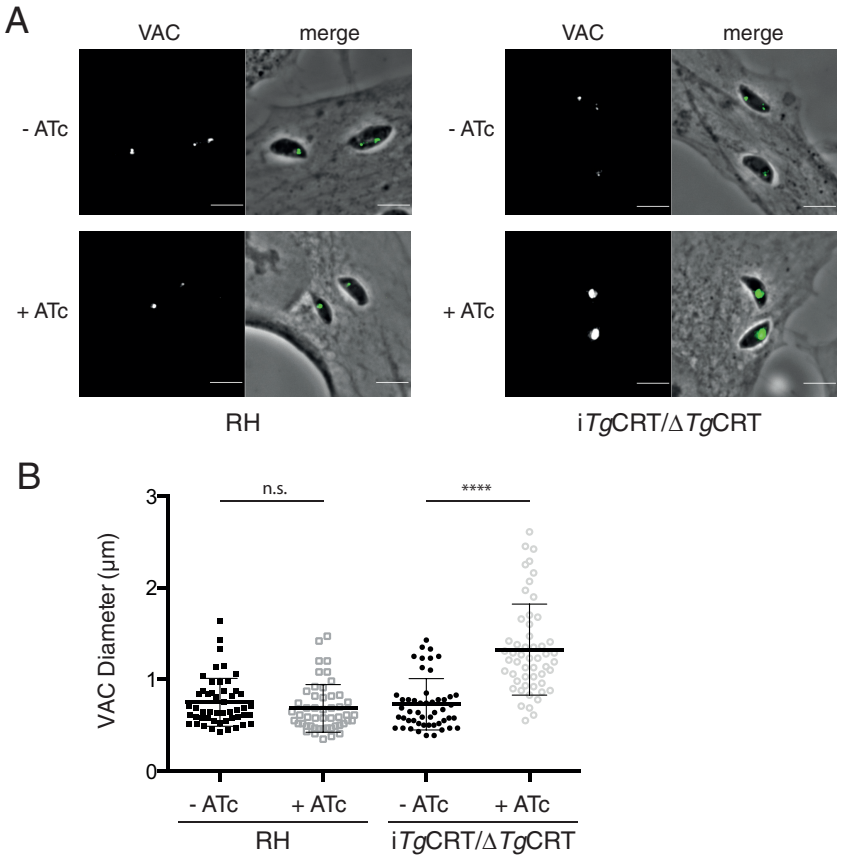

FIG 7 Loss of *Tg*CRT results in swelling of the VAC. (A) Representative images of wild-type (RH) and i*Tg*CRT/Δ*Tg*CRT parasites grown in the absence and presence of ATc and labeled with anti-CPL antibodies to highlight the VAC. (B) Quantification of VAC diameters in wild-type and i*Tg*CRT/Δ*Tg*CRT parasites grown in the presence and absence of ATc. ****, $P < 0.0001$; n.s., not significant.

resistance to chloroquine and led to an alkalinization of the DV (30), suggesting a possible role for CRT in acidification of this compartment. Plant chloroquine-like transporters function in transporting glutathione, and a recent study implicates chloroquine-resistant *Pf*CRT (but not chloroquine-sensitive *Pf*CRT) in glutathione transport into the DV (10, 44).

In this study, we demonstrate that TgCRT is not essential for the growth of *T. gondii* under standard *in vitro* culture conditions. Although our data suggest robust knockdown of *Tg*CRT in the i*Tg*CRT/Δ*Tg*CRT parasite line compared to wild-type levels (Fig. 6B), we cannot rule out that a small amount of *Tg*CRT is expressed that is sufficient for *Tg*CRT function. Nevertheless,

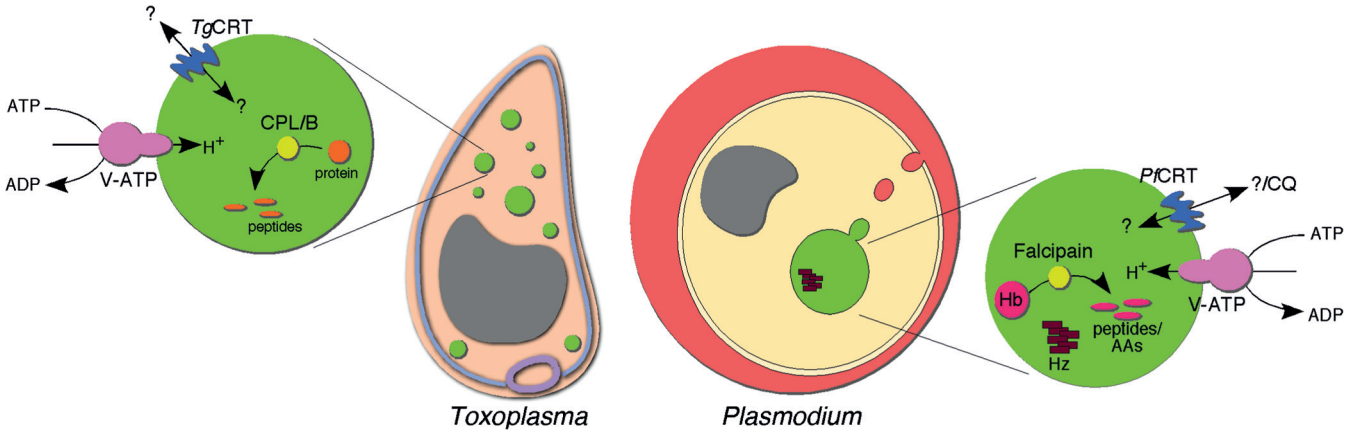

FIG 8 Similarities between the VAC compartment of *T. gondii* and the digestive vacuole of *Plasmodium*. In addition to the presence of CRT family proteins, both the VAC and digestive vacuole contain cathepsin-like cysteine proteases, such as the *Plasmodium* falcipains, *Tg*CPL and *Tg*CPB. Both compartments are acidic, with this acidity maintained through the function of a V-type H^+-pumping ATPase (V-ATP). CQ, chloroquine; Hb, hemoglobin; Hz, hemozoin.

competition growth assays revealed that the loss of TgCRT imparts a fitness cost to the parasite. Intriguingly, a reduction in *Tg*CRT levels results in an enlargement of the VAC compartment. The reasons for this remain unclear. It is possible that *Tg*CRT has a role in the biogenesis or homeostasis of the VAC. For example, the loss of *Tg*CRT may influence the pH of the VAC (much like depletion of *Pf*CRT alters the pH in the DV of *Plasmodium* [30]), which in turn could influence ion regulation and lead to swelling of the organelle. Notably, we have previously demonstrated that treatment of *T. gondii* with agents that cause alkalinization of acidic compartments (bafilomycin A1, which inhibits V-type H^+-ATPases, and chloroquine) disrupts some of the functions of the VAC and leads to swelling of this compartment (11).

It is equally possible that the loss of *Tg*CRT leads to an accumulation of the native substrate transported by *Tg*CRT, which in turn causes VAC swelling. Another possibility is that *Tg*CRT, like plant chloroquine-like transporters and chloroquine resistance alleles of *Pf*CRT (10, 44), has a role in transporting glutathione. Dysregulation of glutathione functions in the VAC may then lead to the swelling of this organelle.

P. falciparum parasites harboring chloroquine resistance alleles of *Pf*CRT are less fit than strains with chloroquine-sensitive *Pf*CRT. Cessation of chloroquine treatment in areas where chloroquine resistance is prevalent frequently leads to the reemergence of chloroquine-sensitive *P. falciparum* strains (e.g., see reference 45). More recently, this reemergence has been duplicated in a laboratory environment (46). The latter study performed competition growth assays with chloroquine-sensitive and -resistant strains of *P. falciparum* in the absence of chloroquine. The study found that chloroquine-sensitive strains almost entirely outcompeted resistant strains over an ~70-day time frame (46). This mirrors our findings with *T. gondii* parasites that were depleted of *Tg*CRT. The same study examined the metabolic differences between chloroquine-sensitive and -resistant strains of *P. falciparum* and found that parasites harboring chloroquine resistance alleles accumulated hemoglobin-derived peptides (46). This suggests that parasites carrying mutated forms of *Pf*CRT are less efficient in catabolizing hemoglobin, which may in turn affect parasite amino acid pools and result in the observed decrease in fitness.

Less clear is how these observed phenotypes correspond to the function of *Pf*CRT (46). As we have proposed for the effects of the *Tg*CRT mutant on VAC function, it is possible that mutated forms of *Pf*CRT perturbed DV function and this led to impairment of hemoglobin digestion. Another possibility is that *Pf*CRT functions as a peptide (or amino acid) transporter, with impairment of the transporter then leading to the accumulation of peptides in the DV. In this context, it is certainly intriguing that glutathione, which is transported by plant chloroquine-like transporters (10), is a tripeptide. Could *Tg*CRT be functioning as a peptide or amino acid transporter? Given the presence of proteases like *Tg*CPL and *Tg*CPB, it is conceivable that one function of the VAC is in protein catabolism, with peptides or amino acids derived from this process contributing to overall parasite amino acid pools. *T. gondii* is auxotrophic for many amino acids (47), which are primarily derived from the growth medium by *in vitro* cultures. We tested whether *Tg*CRT knockdown parasites had impaired growth in amino acid-depleted medium but observed no differences compared to the growth of parasites that expressed *Tg*CRT (not shown). This does not rule out the possibility that *Tg*CRT functions as a peptide or amino acid transporter—it could be that the contribution of the VAC to overall amino acid pools is minimal or that peptide or amino acid transport from the VAC is important to maintain VAC functions.

In this study, we have examined the localization and possible functions of *Tg*CRT, with a view to elucidating the origin and evolution of CRT family proteins. CRT family proteins localize to lysosome-like vacuolar organelles in both *T.* gondii and *Plasmodium*. In *T. gondii*, the VAC compartment to which *Tg*CRT localizes is a highly dynamic structure, potentially involved in numerous roles within the parasite. CRT family proteins exist in a range of other organisms, presenting opportunities to further explore the function(s) of this important group of transporters.

ACKNOWLEDGMENTS

We thank Tracey Schultz and Kelly Rogers for technical assistance, Gary Ward, Chris Tonkin, Nick Katris, Gustavo Arrizabalaga, and Silvia Moreno for providing reagents, and Harpreet Vohra for performing flow cytometry.

This work was supported by an Early Career Researcher grant from the University of Melbourne and an Australian Research Council grant (DP110103144) to G.G.V.D., an Australian National Health and Medical Council Program grant to G.I.M., and a U.S. National Institutes of Health grant (AI063263) to V.B.C. G.G.V.D is a QEII Fellow of the Australian Research Council.

REFERENCES

1. **Liu J, Istvan ES, Gluzman IY, Gross J, Goldberg DE.** 2006. *Plasmodium falciparum* ensures its amino acid supply with multiple acquisition pathways and redundant proteolytic enzyme systems. Proc. Natl. Acad. Sci. U. S. A. **103:**8840–8845. http://dx.doi.org/10.1073/pnas.0601876103.
2. **Goldberg DE, Slater AF, Cerami A, Henderson GB.** 1990. Hemoglobin degradation in the malaria parasite *Plasmodium falciparum*: an ordered process in a unique organelle. Proc. Natl. Acad. Sci. U. S. A. **87:**2931–2935. http://dx.doi.org/10.1073/pnas.87.8.2931.
3. **Pagola S, Stephens PW, Bohle DS, Kosar AD, Madsen SK.** 2000. The structure of malaria pigment beta-haematin. Nature **404:**307–310. http://dx.doi.org/10.1038/35005132.
4. **Slater AF, Cerami A.** 1992. Inhibition by chloroquine of a novel haem polymerase enzyme activity in malaria trophozoites. Nature **355:**167–169. http://dx.doi.org/10.1038/355167a0.
5. **Fidock DA, Nomura T, Talley AK, Cooper RA, Dzekunov SM, Ferdig MT, Ursos LM, Sidhu AB, Naude B, Deitsch KW, Su XZ, Wootton JC, Roepe PD, Wellems TE.** 2000. Mutations in the *P. falciparum* digestive vacuole transmembrane protein *Pf*CRT and evidence for their role in chloroquine resistance. Mol. Cell **6:**861–871. http://dx.doi.org/10.1016/S1097-2765(05)00077-8.
6. **Wellems TE, Panton LJ, Gluzman IY, do Rosario VE, Gwadz RW, Walker-Jonah A, Krogstad DJ.** 1990. Chloroquine resistance not linked to mdr-like genes in a *Plasmodium falciparum* cross. Nature **345:**253–255. http://dx.doi.org/10.1038/345253a0.
7. **Martin RE, Marchetti RV, Cowan AI, Howitt SM, Broer S, Kirk K.** 2009. Chloroquine transport via the malaria parasite's chloroquine resistance transporter. Science **325:**1680–1682. http://dx.doi.org/10.1126/science.1175667.
8. **Martin RE, Kirk K.** 2004. The malaria parasite's chloroquine resistance transporter is a member of the drug/metabolite transporter superfamily. Mol. Biol. Evol. **21:**1938–1949. http://dx.doi.org/10.1093/molbev/msh205.
9. **Tran CV, Saier MH, Jr.** 2004. The principal chloroquine resistance protein of *Plasmodium falciparum* is a member of the drug/metabolite transporter superfamily. Microbiology **150:**1–3. http://dx.doi.org/10.1099/mic.0.26818-0.
10. **Maughan SC, Pasternak M, Cairns N, Kiddle G, Brach T, Jarvis R, Haas F, Nieuwland J, Lim B, Muller C, Salcedo-Sora E, Kruse C, Orsel M, Hell R, Miller AJ, Bray P, Foyer CH, Murray JA, Meyer AJ, Cobbett CS.** 2010. Plant homologs of the *Plasmodium falciparum* chloroquine-resistance transporter, *Pf*CRT, are required for glutathione homeostasis and stress responses. Proc. Natl. Acad. Sci. U. S. A. **107:**2331–2336. http://dx.doi.org/10.1073/pnas.0913689107.

11. **Parussini F, Coppens I, Shah PP, Diamond SL, Carruthers VB.** 2010. Cathepsin L occupies a vacuolar compartment and is a protein maturase within the endo/exocytic system of *Toxoplasma gondii*. Mol. Microbiol. **76:**1340–1357. http://dx.doi.org/10.1111/j.1365-2958.2010.07181.x.
12. **Larkin MA, Blackshields G, Brown NP, Chenna R, McGettigan PA, McWilliam H, Valentin F, Wallace IM, Wilm A, Lopez R, Thompson JD, Gibson TJ, Higgins DG.** 2007. Clustal W and Clustal X version 2.0. Bioinformatics **23:**2947–2948. http://dx.doi.org/10.1093/bioinformatics/btm404.
13. **Waterhouse AM, Procter JB, Martin DM, Clamp M, Barton GJ.** 2009. Jalview version 2—a multiple sequence alignment editor and analysis workbench. Bioinformatics **25:**1189–1191. http://dx.doi.org/10.1093/bioinformatics/btp033.
14. **Guindon S, Dufayard JF, Lefort V, Anisimova M, Hordijk W, Gascuel O.** 2010. New algorithms and methods to estimate maximum-likelihood phylogenies: assessing the performance of PhyML 3.0. Syst. Biol. **59:**307–321. http://dx.doi.org/10.1093/sysbio/syq010.
15. **van Dooren GG, Tomova C, Agrawal S, Humbel BM, Striepen B.** 2008. *Toxoplasma gondii* Tic20 is essential for apicoplast protein import. Proc. Natl. Acad. Sci. U. S. A. **105:**13574–13579. http://dx.doi.org/10.1073/pnas.0803862105.
16. **Agrawal S, van Dooren GG, Beatty WL, Striepen B.** 2009. Genetic evidence that an endosymbiont-derived endoplasmic reticulum-associated protein degradation (ERAD) system functions in import of apicoplast proteins. J. Biol. Chem. **284:**33683–33691. http://dx.doi.org/10.1074/jbc.M109.044024.
17. **Carey KL, Donahue CG, Ward GE.** 2000. Identification and molecular characterization of GRA8, a novel, proline-rich, dense granule protein of *Toxoplasma gondii*. Mol. Biochem. Parasitol. **105:**25–37. http://dx.doi.org/10.1016/S0166-6851(99)00160-7.
18. **Alexandrov A, Vignali M, LaCount DJ, Quartley E, de Vries C, De Rosa D, Babulski J, Mitchell SF, Schoenfeld LW, Fields S, Hol WG, Dumont ME, Phizicky EM, Grayhack EJ.** 2004. A facile method for high-throughput co-expression of protein pairs. Mol. Cell. Proteomics **3:**934–938. http://dx.doi.org/10.1074/mcp.T400008-MCP200.
19. **Brydges SD, Sherman GD, Nockemann S, Loyens A, Daubener W, Dubremetz JF, Carruthers VB.** 2000. Molecular characterization of TgMIC5, a proteolytically processed antigen secreted from the micronemes of *Toxoplasma gondii*. Mol. Biochem. Parasitol. **111:**51–66. http://dx.doi.org/10.1016/S0166-6851(00)00296-6.
20. **Bogdanov AM, Bogdanova EA, Chudakov DM, Gorodnicheva TV, Lukyanov S, Lukyanov KA.** 2009. Cell culture medium affects GFP photostability: a solution. Nat. Methods **6:**859–860. http://dx.doi.org/10.1038/nmeth1209-859.
21. **Gubbels MJ, Li C, Striepen B.** 2003. High-throughput growth assay for *Toxoplasma gondii* using yellow fluorescent protein. Antimicrob. Agents Chemother. **47:**309–316. http://dx.doi.org/10.1128/AAC.47.1.309-316.2003.
22. **Naude B, Brzostowski JA, Kimmel AR, Wellems TE.** 2005. *Dictyostelium discoideum* expresses a malaria chloroquine resistance mechanism upon transfection with mutant, but not wild-type, *Plasmodium falciparum* transporter *Pf*CRT. J. Biol. Chem. **280:**25596–25603. http://dx.doi.org/10.1074/jbc.M503227200.
23. **Summers RL, Dave A, Dolstra TJ, Bellanca S, Marchetti RV, Nash MN, Richards SN, Goh V, Schenk RL, Stein WD, Kirk K, Sanchez CP, Lanzer M, Martin RE.** 2014. Diverse mutational pathways converge on saturable chloroquine transport via the malaria parasite's chloroquine resistance transporter. Proc. Natl. Acad. Sci. U. S. A. **111:**E1759–E1767. http://dx.doi.org/10.1073/pnas.1322965111.
24. **Huynh MH, Carruthers VB.** 2009. Tagging of endogenous genes in a *Toxoplasma gondii* strain lacking Ku80. Eukaryot. Cell **8:**530–539. http://dx.doi.org/10.1128/EC.00358-08.
25. **Fox BA, Ristuccia JG, Gigley JP, Bzik DJ.** 2009. Efficient gene replacements in *Toxoplasma gondii* strains deficient for nonhomologous end joining. Eukaryot. Cell **8:**520–529. http://dx.doi.org/10.1128/EC.00357-08.
26. **Fujiki Y, Hubbard AL, Fowler S, Lazarow PB.** 1982. Isolation of intracellular membranes by means of sodium carbonate treatment: application to endoplasmic reticulum. J. Cell Biol. **93:**97–102. http://dx.doi.org/10.1083/jcb.93.1.97.
27. **Moreno SN, Zhong L, Lu HG, Souza WD, Benchimol M.** 1998. Vacuolar-type H^+-ATPase regulates cytoplasmic pH in *Toxoplasma gondii* tachyzoites. Biochem. J. **330**(Pt 2)**:**853–860.
28. **Miranda K, Pace DA, Cintron R, Rodrigues JC, Fang J, Smith A, Rohloff P, Coelho E, de Haas F, de Souza W, Coppens I, Sibley LD, Moreno SN.** 2010. Characterization of a novel organelle in *Toxoplasma gondii* with similar composition and function to the plant vacuole. Mol. Microbiol. **76:**1358–1375. http://dx.doi.org/10.1111/j.1365-2958.2010.07165.x.
29. **Francia ME, Wicher S, Pace DA, Sullivan J, Moreno SN, Arrizabalaga G.** 2011. A Toxoplasma gondii protein with homology to intracellular type Na^+/H^+ exchangers is important for osmoregulation and invasion. Exp. Cell Res. **317:**1382–1396. http://dx.doi.org/10.1016/j.yexcr.2011.03.020.
30. **Waller KL, Muhle RA, Ursos LM, Horrocks P, Verdier-Pinard D, Sidhu AB, Fujioka H, Roepe PD, Fidock DA.** 2003. Chloroquine resistance modulated in vitro by expression levels of the *Plasmodium falciparum* chloroquine resistance transporter. J. Biol. Chem. **278:**33593–33601. http://dx.doi.org/10.1074/jbc.M302215200.
31. **Meissner M, Schluter D, Soldati D.** 2002. Role of *Toxoplasma gondii* myosin A in powering parasite gliding and host cell invasion. Science **298:**837–840. http://dx.doi.org/10.1126/science.1074553.
32. **Brooks CF, Johnsen H, van Dooren GG, Muthalagi M, Lin SS, Bohne W, Fischer K, Striepen B.** 2010. The *Toxoplasma* apicoplast phosphate translocator links cytosolic and apicoplast metabolism and is essential for parasite survival. Cell Host Microbe **7:**62–73. http://dx.doi.org/10.1016/j.chom.2009.12.002.
33. **Francis SE, Sullivan DJ, Jr, Goldberg DE.** 1997. Hemoglobin metabolism in the malaria parasite *Plasmodium falciparum*. Annu. Rev. Microbiol. **51:**97–123. http://dx.doi.org/10.1146/annurev.micro.51.1.97.
34. **van Dooren GG, Ralph SA.** 2010. Novel vacuoles in *Toxoplasma*. Mol. Microbiol. **76:**1335–1339. http://dx.doi.org/10.1111/j.1365-2958.2010.07197.x.
35. **Sullivan DJ, Jr, Gluzman IY, Russell DG, Goldberg DE.** 1996. On the molecular mechanism of chloroquine's antimalarial action. Proc. Natl. Acad. Sci. U. S. A. **93:**11865–11870. http://dx.doi.org/10.1073/pnas.93.21.11865.
36. **van Dooren GG, Kennedy AT, McFadden GI.** 2012. The use and abuse of heme in apicomplexan parasites. Antioxid. Redox Signal. **17:**634–656. http://dx.doi.org/10.1089/ars.2012.4539.
37. **Macomber PB, Sprinz H.** 1967. Morphological effects of chloroquine on *Plasmodium berghei* in mice. Nature **214:**937–939. http://dx.doi.org/10.1038/214937a0.
38. **Warhurst DC, Hockley DJ.** 1967. Mode of action of chloroquine on *Plasmodium berghei* and *P. cynomolgi*. Nature **214:**935–936. http://dx.doi.org/10.1038/214935a0.
39. **Dou Z, Coppens I, Carruthers VB.** 2013. Noncanonical maturation of two papain-family proteases in *Toxoplasma gondii*. J. Biol. Chem. **288:**3523–3534. http://dx.doi.org/10.1074/jbc.M112.443697.
40. **Dou Z, Carruthers VB.** 2011. Cathepsin proteases in *Toxoplasma gondii*. Adv. Exp. Med. Biol. **712:**49–61. http://dx.doi.org/10.1007/978-1-4419-8414-2_4.
41. **Hayashi M, Yamada H, Mitamura T, Horii T, Yamamoto A, Moriyama Y.** 2000. Vacuolar H^+-ATPase localized in plasma membranes of malaria parasite cells, Plasmodium falciparum, is involved in regional acidification of parasitized erythrocytes. J. Biol. Chem. **275:**34353–34358. http://dx.doi.org/10.1074/jbc.M003323200.
42. **Abu Bakar N, Klonis N, Hanssen E, Chan C, Tilley L.** 2010. Digestive-vacuole genesis and endocytic processes in the early intraerythrocytic stages of *Plasmodium falciparum*. J. Cell Sci. **123:**441–450. http://dx.doi.org/10.1242/jcs.061499.
43. **Drew ME, Banerjee R, Uffman EW, Gilbertson S, Rosenthal PJ, Goldberg DE.** 2008. *Plasmodium* food vacuole plasmepsins are activated by falcipains. J. Biol. Chem. **283:**12870–12876. http://dx.doi.org/10.1074/jbc.M708949200.
44. **Patzewitz EM, Salcedo-Sora JE, Wong EH, Sethia S, Stocks PA, Maughan SC, Murray JA, Krishna S, Bray PG, Ward SA, Muller S.** 2013. Glutathione transport: a new role for *Pf*CRT in chloroquine resistance. Antioxid. Redox Signal. **19:**683–695. http://dx.doi.org/10.1089/ars.2012.4625.
45. **Kublin JG, Cortese JF, Njunju EM, Mukadam RA, Wirima JJ, Kazembe PN, Djimde AA, Kouriba B, Taylor TE, Plowe CV.** 2003. Reemergence of chloroquine-sensitive *Plasmodium falciparum* malaria after cessation of chloroquine use in Malawi. J. Infect. Dis. **187:**1870–1875. http://dx.doi.org/10.1086/375419.
46. **Lewis IA, Wacker M, Olszewski KL, Cobbold SA, Baska KS, Tan A, Ferdig MT, Llinas M.** 2014. Metabolic QTL analysis links chloroquine resistance in *Plasmodium falciparum* to impaired hemoglobin catabolism. PLoS Genet. **10:**e1004085. http://dx.doi.org/10.1371/journal.pgen.1004085.
47. **Coppens I.** 2014. Exploitation of auxotrophies and metabolic defects in *Toxoplasma* as therapeutic approaches. Int. J. Parasitol. **44:**109–120. http://dx.doi.org/10.1016/j.ijpara.2013.09.003.